Frequency-Multiplexed Photon Pairs Over 1000 Modes from a Quadratic Nonlinear Optical Waveguide Resonator with a Singly Resonant Configuration

Rikizo Ikuta,[1,2] Ryoya Tani,[1] Masahiro Ishizaki,[1] Shigehito Miki,[3,4] Masahiro Yabuno,[3] Hirotaka Terai,[3] Nobuyuki Imoto,[2] and Takashi Yamamoto[1,2]

[1]*Graduate School of Engineering Science, Osaka University, Toyonaka, Osaka 560-8531, Japan*

[2]*Quantum Information and Quantum Biology Division, Institute for Open and Transdisciplinary Research Initiatives, Osaka University, Osaka 560-8531, Japan*

[3]*Advanced ICT Research Institute, National Institute of Information and Communications Technology (NICT), Kobe 651-2492, Japan*

[4]*Graduate School of Engineering Faculty of Engineering, Kobe University, Kobe 657-0013, Japan*

(Received 23 April 2019; published 8 November 2019)

We demonstrate a frequency multiplexed photon pair generation based on a quadratic nonlinear optical waveguide inside a cavity which confines only signal photons without confining idler photons and the pump light. We monolithically constructed the photon pair generator by a periodically poled lithium niobate (PPLN) waveguide with a high reflective coating for the signal photons around 1600 nm and with antireflective coatings for the idler photons around 1520 nm and the pump light at 780 nm at the end faces of the PPLN waveguide. We observed a comblike photon pair generation with a mode spacing of the free spectral range of the cavity. Unlike the conventional multiple resonant photon pair generation experiments, the photon pair generation was incessant within a range of 80 nm without missing teeth due to a mismatch of the energy conservation and the cavity resonance condition of the photons, resulting in over 1000-mode frequency multiplexed photon pairs in this range.

DOI: 10.1103/PhysRevLett.123.193603

Photon pairs produced by spontaneous parametric down-conversion (SPDC) or spontaneous four wave mixing are commonly used as a resource of single photons and entangled photon pairs in photonic quantum information experiments. Unfortunately, the photon pairs include not only the genuine single photon pair but also multiple photon pair emission, which degrades the quality of the single-photon-based experiments. Typically, suppression of the multiple photon emission is achieved by setting a single photon emission probability to a value much smaller than unity, while it makes the amount of the vacuum large and the success probability of the protocol small. To boost the success probability without increasing the photon emission rate per mode, parallel processing of the protocol [1,2] or use of a larger Hilbert space [3,4] is effective. For this purpose, frequency multiplexed photon pair generation has been actively studied. Such a photon pair generator can be realized by using an optical parametric oscillator (OPO) far below threshold [5]. A nonlinear optical medium is installed in an optical cavity for confining the photons, and a sufficiently weak pump light for the photon pair generation is used. Typical nonlinear optical media have a wide bandwidth for photon pair generation, whereas the optical cavity suppresses the photon generation in nonresonant modes. As a result, photon pairs with clear frequency mode separation are produced. So far, a lot of experiments of the photon pair generation with various cavity configurations have been performed [1,6] by the quadratic nonlinearity with an external cavity [7,8], a quadratic nonlinearity-based microring resonator [9], and Kerr nonlinearity-based microring resonators [4,10–15]. However, to the best of our knowledge, all of the previous demonstrations for frequency multiplexed photon pair generation have used a doubly resonant OPO which confines both the signal and the idler photons, or a triply resonant OPO which additionally confines the pump light. While the photon pair generation by using a singly resonant (SR) OPO which confines only one half of the photon pair has been demonstrated in Ref. [16], the experiment focused on the narrow-band single photon generation as in the case of the photon pair generation by the doubly resonant OPO [17–25].

In this Letter, we demonstrate a frequency multiplexed photon pair generation based on a quadratic nonlinear optical medium with the SR OPO configuration. In the experiment, we used a periodically poled lithium niobate (PPLN) waveguide as the nonlinear optical medium which is widely used in the quantum information experiments [26,27] and has a possibility to integrate into an on-chip photonic circuit [27–31]. In our experiment, a pair of photons is generated into a long and a short wavelength comblike mode. For convenience, we call the long one and the short one as signal and idler photon, respectively. Our cavity is designed for confining only the signal photons in a monolithically integrated quadratic nonlinear waveguide resonator (QNWR) which we call PPLN-QNWR; dielectric

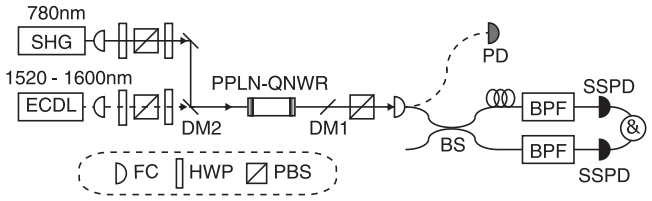

FIG. 1. Our experimental setup for photon pair generation. DM2 reflects the 780-nm light and transmits the telecom photons. FC is a fiber coupler.

multilayers are directly formed at the end faces of the PPLN waveguide. The photon pair generation with the SR configuration has several features as follows. The photon pair generator does not need a severe stabilization of the pump laser frequency to the cavity. In addition, in spite of no cavity configuration for the idler photons, not only the signal photons but also the idler photons have comblike spectrum as if both of them are confined in the cavity. Different from the photon pairs by the multiple resonant OPO, the spectra in SR configuration do not have missing teeth within specific spectral intervals derived from a mismatch of the energy conservation and the cavity resonance conditions of the photons known as the cluster effect [19,21–24] (see Supplemental Material [32]).

As a result, a wide-band frequency multiplexed photon pair generation can be possible. When we regard the device as a single photon generator in the idler mode heralded by the signal photon of the photon pair, the idler photon does not suffer from the cavity loss and thus the narrow spectral photon can be efficiently prepared. The heralded idler photon has an exponential rising waveform as the time reversed waveform of the heralding signal photon confined in the cavity. This property is expected to achieve a high mode matching to an atomic resonance [36,37] like the narrow-band photons via spontaneous four-wave mixing in atoms [38,39] and optical circuits employing cavity systems [40,41].

The experimental setup is shown in Fig. 1. A continuous wave pump light at 780 nm for SPDC is frequency stabilized to a resonance of rubidium atoms [42]. By using a pair of half-wave plates (HWP) sandwiching a polarization beam splitter (PBS), the power of the pump light coupled to the waveguide is set to 500 μW to 2 mW, and its polarization is set to vertical (V) polarization. After that, the pump light is focused on the PPLN-QNWR for SPDC with the coupling efficiency of 0.9.

The PPLN waveguide used in our experiment is a zinc-doped lithium niobate as a core and lithium tantalite as a clad. The length is 20 mm. The periodically poling period is 18.090 nm, and the waveguide satisfies the type-0 quasi-phase matching (the polarization of the relevant three light is V) of the second harmonic generation of 1560-nm light at 50 °C. Both ends of the PPLN are flat polished for Fabry-Pérot cavity structure, and coated by the dielectric

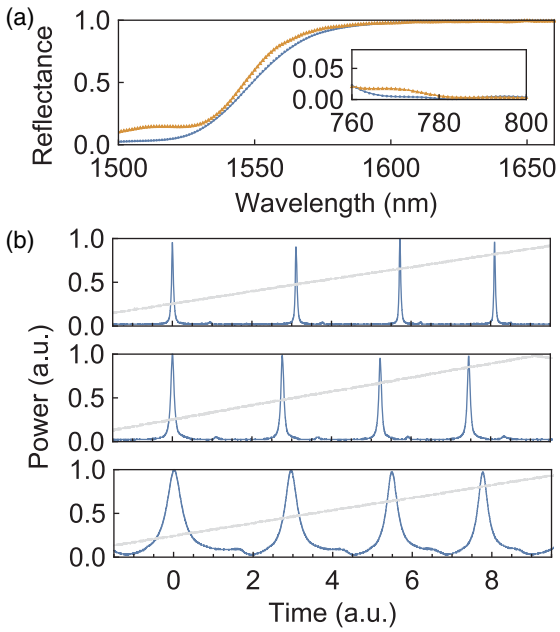

FIG. 2. (a) Reflectances of the coating at the surfaces of lithium niobate samples coated at the same batches for the PPLN waveguide. The inset shows the reflectances for around the pump wavelength. The orange and the blue curves are for the back and the front ends of the PPLN, respectively. (b) Observed power of the light passing through the PPLN-QNWR for 1600, 1580, and 1560 nm light from the top. The gray lines describe voltages applied to the ECDL for the wavelength sweep. Each peak is fitted by a function $A[(f-f_0)^2+(\gamma_f/2)^2]^{-1}+d$ with fitting parameters A, f_0, γ_f, and d.

multilayers for a high reflective coating around 1600 nm and antireflective coatings around 1520 nm and 780 nm, which are shown in Fig. 2(a). The signal and the idler photons generated at the PPLN-QNWR are separated from the pump light by a dichroic mirror (DM1), and then the V-polarized photons are coupled to a single mode fiber (SMF). The photons are divided into two paths by a fiber-based half beam splitter. Both photons pass through bandpass filters (BPF) with their minimum bandwidth of 0.03 nm, and finally they are detected by superconducting single photon detectors (SSPDs) [43]. The electrical signals from the two detectors are connected to the time-to-digital converter (TDC), and the coincidence counts with time stamps are recorded.

Before the photon-pair generation, we first measured the optical response of the PPLN-QNWR. We turn off the pump laser at 780 nm, and we observe the transmission spectra of a telecom light from an external cavity diode laser (ECDL) with scanning the frequency. The telecom light output from the PPLN-QNWR is coupled to the SMF, and is detected by a photo detector (PD) followed by an oscilloscope. Examples of the observed resonant peaks are shown in Fig. 2(b). Each peak is fitted by using a Lorentzian with a constant noise level. By borrowing the free spectral range (FSR) $\Delta_f = 3.5$ GHz of the cavity from

TABLE I. The estimated FWHM γ_f of the resonant peaks.

Wavelength	FWHM γ_f	Q factor	Finesse
1600 nm	60 MHz	3.2×10^6	59
1580 nm	116 MHz	1.6×10^6	29
1560 nm	470 MHz	0.4×10^6	7

a previous reported value by using a 20-mm-long PPLN waveguide with a resonant structure for telecom light [44], we showed a full width at the half maximum (FWHM) denoted by γ_f in Table I.

From the above experimental result, the photon pairs in the SR configuration are expected to be generated with their mode spacing corresponding to FSR of the cavity. To see this, we measured the beat signals of the frequency separated photons by the coincidence measurement. We set the bandwidths of the BPFs to 1 nm for collecting the several separated frequency modes for both the signal and the idler photons. The electrical signals from the detectors for the idler and the signal photons are used as a start and a stop of the TDC, respectively. In this setup, the beat effect among the frequencies of the detected photons should be observed as an oscillation of the coincidence counts between the signal and the idler photons [16,33] (and also see Eqs. (15) and (17) in Ref. [32]). In Fig. 3 from the top, We show the experimental results for signal and idler pairs in SR configuration around 1600 and 1522 nm and 1580 and 1540 nm, and as a reference, the degenerated photon pair around 1560 nm in doubly resonant configuration. From the figure, we clearly observed the oscillation of the coincidence, which indicates that the photon pairs are in a superposition of different frequency modes with a mode spacing. By picking up the peaks of the observed coincidence, we calculated the periodic time of the peaks about the photon pairs around 1600 and 1522 nm, 1580 and 1540 nm, and 1560 and 1560 nm. The estimated time periods are 286, 286, and 282 ps, respectively, that correspond to the FSR $\Delta_f = 3.5$ GHz of the cavity. This shows that the photon pairs were surely produced with a mode spacing of the FSR.

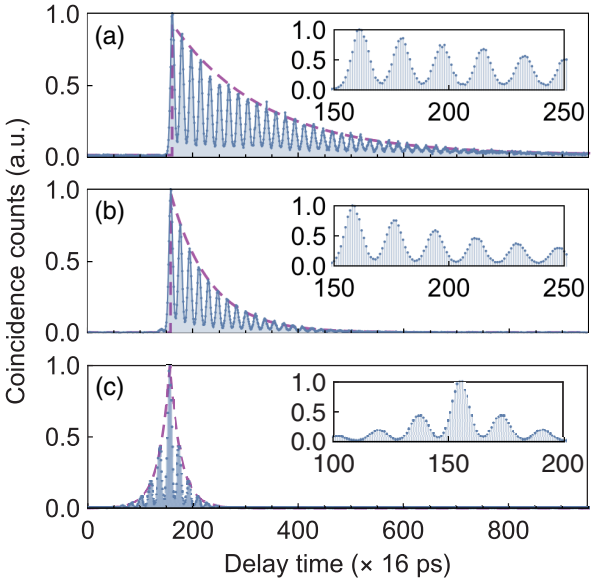

FIG. 3. Observed coincidence counts with the filter bandwidths of 1 nm. The wavelengths of the signal and the idler photons are (a) 1600 nm and 1522 nm and (b) 1580 nm and 1540 nm. (c) The case of the degenerated photon pair around 1560 nm. The non zero values of the minimum of the fringes is caused by the timing jitter about 80 ps of the SSPDs.

In Fig. 3, we see not only the oscillation but also the time decay of the coincidence counts. In the case of the doubly resonant photon pair around 1560 nm, the symmetric waveform in the time domain was observed as in the previous experiments [18,23]. On the other hand, in the cases of the photon pairs in SR configuration around 1600 and 1522 nm and 1580 and 1540 nm, single-sided exponential time decays were observed. The best fit of the envelopes of the curves to the Lorentzian $A\exp[-\gamma(t-\tau_0)/2]+d$ for $t \geq \tau_0$ and d for $t < \tau_0$ with fitting parameters A, γ, and d shows that the FWHMs $\gamma/(2\pi)$ of the Lorentzian in the frequency domain are 114 and 270 MHz, respectively. Here τ_0 is the time when the maximum of the coincidence counts was obtained. The values are almost twice as large as the FWHMs γ_f estimated by using the classical laser light in Table I. This is in good agreement with theoretical analysis in Eqs. (2) and (15) in Ref. [32].

Next we set the bandwidth of the BPFs for the signal and idler photons to 0.03 nm corresponds to 3.7 GHz. These filters severely limit the frequency modes to a single mode for both signal and idler. We set the center wavelengths of the BPFs to 1600 and 1522 nm. The observed coincidence counts are shown in Fig. 4. Becuase of the single frequency mode filtering, the exponential time decay without oscillation was observed. By swapping the role of the BPFs, the coincidence counts with the time reversed shape was obtained. The origin of the difference is referred in Eqs. (15) and (17) in Ref. [32]. This result can be interpreted that the

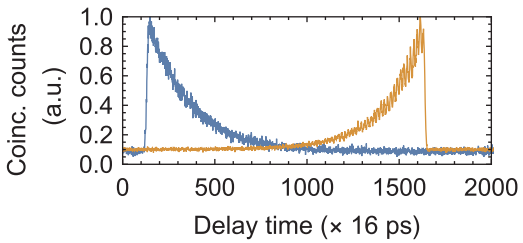

FIG. 4. The coincidence counts with exponential decay (rising) described by blue (orange) show the signal (idler) photon counts heralded by the idler (signal) photons of the photon pair. The measurement was performed with the bandwidths 0.03 nm of the BPFs.

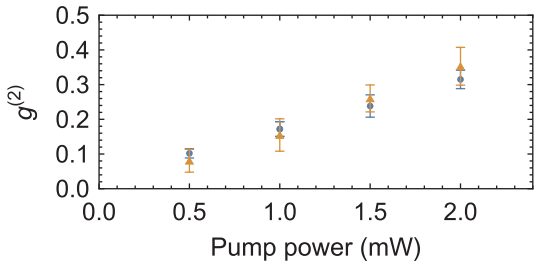

FIG. 5. $g^{(2)}$ vs pump power. The blue circles are about signal photons heralded by idle photons, and the orange triangles are about idler photons heralded by signal photons.

photon with the exponential rising shape is prepared in the idler mode heralded by the signal photon detection.

For the above wavelengh setting, we measured the second-order intensity correlation function $g^{(2)}$ of the signal (idler) photon heralded by the idler (signal) photon. The measurement was performed by splitting photons into two spatial paths after one of the BPFs in Fig. 1. The coincidence time window was set to 9 ns (corresponding to ~560 bin in Fig. 4), in which a large portion of the wave packet was included. The experimental result is shown in Fig. 5. As is the case with the conventional SPDC process, the functions $g^{(2)}$ of the heralded signal and idler photons take the same value, and are proportional to the pump power in this power range.

The single and coincidence counts are also proportional to the pump power as shown in Fig. 6. The ratio of the single counts of the signal photons to that of the idler photons is about 0.54. The coupling efficiencies of the signal and the idler photons were estimated to be almost the same by using the classical laser light, and thus the difference of the single counts reflects our cavity design such that the reflectance at the both ends of the PPLN-QNWR for 1600 nm is the same as shown in Fig. 2(a). If a proper high reflective coating is formed at the front end of

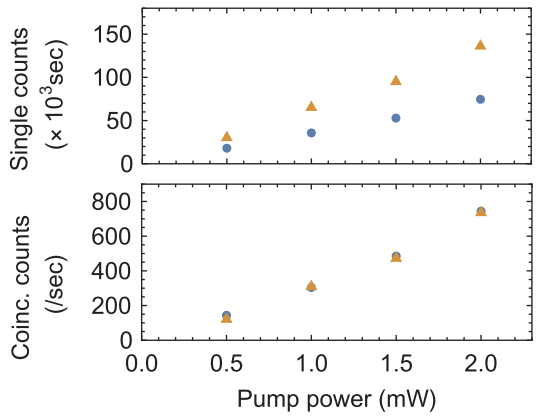

FIG. 6. Pump dependencies of single counts of signal photons (blue circles) and idler photons (orange triangles), and coincidence counts when signal (idler) photons are used as start of TDC which are plotted by blue circles (orange triangles).

the PPLN, all signal photons will come out from the back end of the PPLN. From the ratio of the coincidence counts to the single counts of the signal (idler) photon, we estimated the transmittance of the optical circuit for the idler (signal) photon. The estimated overall transmittances for the signal and the idler photons just before the photon detectors are 0.009 and 0.013, respectively, with an assumption of the quantum efficiency 0.6 of the SSPDs. The values agree well with those measured by using classical laser light, in which the fiber coupling and frequency filtering efficiencies were 0.3 and 0.05. As a result, the intrinsic photon pair rate emitted from the back end of the PPLN-QNWR within the single resonant pair for 1600 and 1522 nm is estimated as 4×10^6 pairs/(s mW).

Finally, in order to see no cluster effect in the photon pairs produced by the PPLN-QNWR with SR configuration, we removed the BS in Fig. 1, and measured the single photon counts by scanning the center wavelengths of the BPF. The bandwidth of the BPF is set to 3 nm and the pump power is set to 500 μW. The experimental result is shown in Fig. 7. Different from the cases of the SPDC based on the doubly resonant cavity [19,21], the photon pairs were not suppressed over all the spectral range from 1520 to 1600 nm. The expected number of the photon pair modes with the mode spacing of the FSR is about 1400 in this range. We note that the single photon counts for longer wavelengths are smaller, because of our asymmetric cavity design for the signal and the idler photons as is the case with Fig. 6(a).

In conclusion, we have demonstrated the frequency multiplexed photon pair generation based on the PPLN waveguide as the nonlinear optical crystal with the SR OPO configuration in which only signal photons are confined. As is the cases of the photon pair generation based on the multiple resonant OPO, we observed the oscillation of the coincidence counts between the signal and the idler photons. This shows that the frequency modes of the photon pairs are well separated with the mode spacing corresponding to the FSR of the cavity as if both photons are confined in the cavity. The comblike spectra of the photons have no missing teeth due to the elimination of the cluster effect which is seen in the photon pairs based on the PPLN crystal in the doubly resonant OPO. By using the signal photon confined in the cavity as the heralding

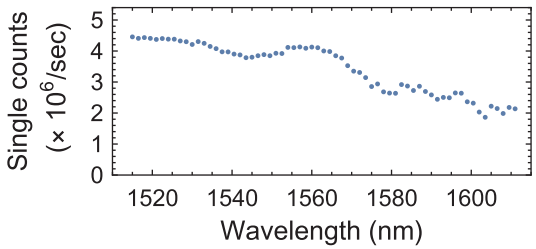

FIG. 7. Observed single counts. The bandwidth of the BPF is set to 3 nm.

photon, the heralded idler photons are efficiently extracted with the exponential rising waveform as the time reversed shape of the heralding signal photons. We believe the wideband frequency multiplexed photon pair generator based on the PPLN waveguide resonator will be useful in various kinds of photonic quantum information processing such as an efficient quantum key distribution [45,46], an efficient photon-matter interface with an atomic frequency comb [47–49]. In addition, the cavity design with different finesses depending on the frequency will be a significant progress for manipulation of the temporal mode [50] and frequency mode [2,3,51–53] with the use of frequency-domain optical elements [54–56].

We thank Motoki Asano and Yoshiaki Tsujimoto for fruitful discussion. This work was supported by CREST, JST JPMJCR1671; MEXT/JSPS KAKENHI Grants No. JP16H02214 and No. JP18K13483; Asahi Glass Foundation, Murata Science Foundation, Fujikura Foundation, and Kayamori Foundation of Information Science Advancement.

[1] L. Caspani, C. Xiong, B. J. Eggleton, D. Bajoni, M. Liscidini, M. Galli, R. Morandotti, and D. J. Moss, Integrated sources of photon quantum states based on nonlinear optics, Light Sci. Appl. **6**, e17100 (2017).
[2] C. Joshi, A. Farsi, S. Clemmen, S. Ramelow, and A. L. Gaeta, Frequency multiplexing for quasi-deterministic heralded single-photon sources, Nat. Commun. **9**, 847 (2018).
[3] Z. Xie *et al.*, Harnessing high-dimensional hyperentanglement through a biphoton frequency comb, Nat. Photonics **9**, 536 (2015).
[4] M. Kues *et al.*, On-chip generation of high-dimensional entangled quantum states and their coherent control, Nature (London) **546**, 622 (2017).
[5] Y. J. Lu and Z. Y. Ou, Optical parametric oscillator far below threshold: Experiment versus theory, Phys. Rev. A **62**, 033804 (2000).
[6] M. Kues, C. Reimer, J. M. Lukens, W. J. Munro, A. M. Weiner, D. J. Moss, and R. Morandotti, Quantum optical microcombs, Nat. Photonics **13**, 170 (2019).
[7] H. Wang, T. Horikiri, and T. Kobayashi, Polarization-entangled mode-locked photons from cavity-enhanced spontaneous parametric down-conversion, Phys. Rev. A **70**, 043804 (2004).
[8] T. Kroh, A. Ahlrichs, B. Sprenger, and O. Benson, Heralded wave packet manipulation and storage of a frequency-converted pair photon at telecom wavelength, Quantum Sci. Technol. **2**, 034007 (2017).
[9] X. Guo, C.-l. Zou, C. Schuck, H. Jung, R. Cheng, and H. X. Tang, Parametric down-conversion photon-pair source on a nanophotonic chip, Light Sci. Appl. **6**, e16249 (2017).
[10] C. Reimer *et al.*, Integrated frequency comb source of heralded single photons, Opt. Express **22**, 6535 (2014).
[11] C. Reimer *et al.*, Generation of multiphoton entangled quantum states by means of integrated frequency combs, Science **351**, 1176 (2016).
[12] F. Mazeas *et al.*, High-quality photonic entanglement for wavelength-multiplexed quantum communication based on a silicon chip, Opt. Express **24**, 28731 (2016).
[13] M. Fujiwara, R. Wakabayashi, M. Sasaki, and M. Takeoka, Wavelength division multiplexed and doubleport pumped time-bin entangled photon pair generation using si ring resonator, Opt. Express **25**, 3445 (2017).
[14] J. A. Jaramillo-Villegas, P. Imany, O. D. Odele, D. E. Leaird, Z.-Y. Ou, M. Qi, and A. M. Weiner, Persistent energy–time entanglement covering multiple resonances of an on-chip biphoton frequency comb, Optica **4**, 655 (2017).
[15] P. Imany, J. A. Jaramillo-Villegas, O. D. Odele, K. Han, D. E. Leaird, J. M. Lukens, P. Lougovski, M. Qi, and A. M. Weiner, 50-GHz-spaced comb of high-dimensional frequency-bin entangled photons from an on-chip silicon nitride microresonator, Opt. Express **26**, 1825 (2018).
[16] M. Scholz, F. Wolfgramm, U. Herzog, and O. Benson, Narrow-band single photons from a single-resonant optical parametric oscillator far below threshold, Appl. Phys. Lett. **91**, 191104 (2007).
[17] X.-H. Bao, Y. Qian, J. Yang, H. Zhang, Z. B. Chen, T. Yang, and J. W. Pan, Generation of Narrow-Band Polarization-Entangled Photon Pairs for Atomic Quantum Memories, Phys. Rev. Lett. **101**, 190501 (2008).
[18] M. Scholz, L. Koch, and O. Benson, Statistics of Narrow-band Single Photons for Quantum Memories Generated by Ultrabright Cavity-Enhanced Parametric Down-Conversion, Phys. Rev. Lett. **102**, 063603 (2009).
[19] E. Pomarico, B. Sanguinetti, N. Gisin, R. Thew, H. Zbinden, G. Schreiber, A. Thomas, and W. Sohler, Waveguide-based opo source of entangled photon pairs, New J. Phys. **11**, 113042 (2009).
[20] J. Yang, X. H. Bao, H. Zhang, S. Chen, C. Z. Peng, Z. B. Chen, and J. W. Pan, Experimental quantum teleportation and multiphoton entanglement via interfering narrowband photon sources, Phys. Rev. A **80**, 042321 (2009).
[21] E. Pomarico, B. Sanguinetti, C. I. Osorio, H. Herrmann, and R. T. Thew, Engineering integrated pure narrowband photon sources, New J. Phys. **14**, 033008 (2012).
[22] C.-S. Chuu, G. Y. Yin, and S. E. Harris, A miniature ultrabright source of temporally long, narrowband biphotons, Appl. Phys. Lett. **101**, 051108 (2012).
[23] J. Fekete, D. Rieländer, M. Cristiani, and H. de Riedmatten, Ultranarrow-band photon-pair source compatible with solid state quantum memories and telecommunication networks, Phys. Rev. Lett. **110**, 220502 (2013).
[24] K.-H. Luo, H. Herrmann, S. Krapick, B. Brecht, R. Ricken, V. Quiring, H. Suche, W. Sohler, and C. Silberhorn, Direct generation of genuine single-longitudinalmode narrowband photon pairs, New J. Phys. **17**, 073039 (2015).
[25] K. Niizeki, K. Ikeda, M. Zheng, X. Xie, K. Okamura, N. Takei, N. Namekata, S. Inoue, H. Kosaka, and T. Horikiri, Ultrabright narrow-band telecom two-photon source for long-distance quantum communication, Appl. Phys. Express **11**, 042801 (2018).
[26] O. Alibart, V. D'Auria, M. De Micheli, F. Doutre, F. Kaiser, L. Labonté, T. Lunghi, É. Picholle, and S. Tanzilli, Quantum photonics at telecom wavelengths based on lithium niobate waveguides, J. Opt. **18**, 104001 (2016).

[27] P. R. Sharapova, K. H. Luo, H. Herrmann, M. Reichelt, T. Meier, and C. Silberhorn, Toolbox for the design of LiNbO3-based passive and active integrated quantum circuits, New J. Phys. **19**, 123009 (2017).
[28] M. Förtsch, J. U. Fürst, C. Wittmann, D. Strekalov, A. Aiello, M. V. Chekhova, C. Silberhorn, G. Leuchs, and C. Marquardt, A versatile source of single photons for quantum information processing, Nat. Commun. **4**, 1818 (2013).
[29] H. Jin, F. M. Liu, P. Xu, J. L. Xia, M. L. Zhong, Y. Yuan, J. W. Zhou, Y. X. Gong, W. Wang, and S. N. Zhu, On-Chip Generation and Manipulation of Entangled Photons Based on Reconfigurable Lithium-Niobate Waveguide Circuits, Phys. Rev. Lett. **113**, 103601 (2014).
[30] P. Vergyris, T. Meany, T. Lunghi, G. Sauder, J. Downes, M. J. Steel, M. J. Withford, O. Alibart, and S. Tanzilli, Onchip generation of heralded photon-number states, Sci. Rep. **6**, 35975 (2016).
[31] L. Sansoni, K. H. Luo, C. Eigner, R. Ricken, V. Quiring, H. Herrmann, and C. Silberhorn, A two-channel, spectrally degenerate polarization entangled source on chip, Quantum Inf. **3**, 5 (2017).
[32] See Supplemental Material at http://link.aps.org/supplemental/10.1103/PhysRevLett.123.193603, which includes Refs. [19,21–24,33–35], for the spectral properties of SPDC photons generated with the doubly resonant and the singly resonant OPO configuration.
[33] U. Herzog, M. Scholz, and O. Benson, Theory of biphoton generation in a single-resonant optical parametric oscillator far below threshold, Phys. Rev. A **77**, 023826 (2008).
[34] Y. Jeronimo-Moreno, S. Rodriguez-Benavides, and A. B. U'Ren, Theory of cavity-enhanced spontaneous parametric downconversion, Laser Phys. **20**, 1221 (2010).
[35] H. Bateman, *Tables of Integral Transforms* (McGraw-Hill Book Company, New York, 1954), Vol. 1.
[36] S. Zhang, C. Liu, S. Zhou, C. S. Chuu, M. M. T. Loy, and S. Du, Coherent Control of Single-Photon Absorption and Reemission in a Two-Level Atomic Ensemble, Phys. Rev. Lett. **109**, 263601 (2012).
[37] B. Srivathsan, G. K. Gulati, A. Cerè, B. Chng, and C. Kurtsiefer, Reversing the Temporal Envelope of a Heralded Single Photon Using a Cavity, Phys. Rev. Lett. **113**, 163601 (2014).
[38] S. Du, P. Kolchin, C. Belthangady, G. Y. Yin, and S. E. Harris, Subnatural Linewidth Biphotons with Controllable Temporal Length, Phys. Rev. Lett. **100**, 183603 (2008).
[39] L. Zhao, X. Guo, C. Liu, Y. Sun, M. M. T. Loy, and S. Du, Photon pairs with coherence time exceeding 1 μs, Optica **1**, 84 (2014).
[40] M. Bader, S. Heugel, A. L. Chekhov, M. Sondermann, and G. Leuchs, Efficient coupling to an optical resonator by exploiting time-reversal symmetry, New J. Phys. **15**, 123008 (2013).
[41] C. Liu, Y. Sun, L. Zhao, S. Zhang, M. M. T. Loy, and S. Du, Efficiently Loading a Single Photon into a singlesided Fabry-Perot Cavity, Phys. Rev. Lett. **113**, 133601 (2014).
[42] Y. Tsujimoto *et al.*, High visibility Hong-Ou-Mandel interference via a time-resolved coincidence measurement, Opt. Express **25**, 12069 (2017).
[43] S. Miki, M. Yabuno, T. Yamashita, and H. Terai, Stable, high-performance operation of a fiber-coupled superconducting nanowire avalanche photon detector, Opt. Express **25**, 6796 (2017).
[44] R. Ikuta, M. Asano, R. Tani, T. Yamamoto, and N. Imoto, Frequency comb generation in a quadratic nonlinear waveguide resonator, Opt. Express **26**, 15551 (2018).
[45] D. Aktas, B. Fedrici, F. Kaiser, T. Lunghi, L. Labonté, and S. Tanzilli, Entanglement distribution over 150 km in wavelength division multiplexed channels for quantum cryptography, Laser Photonics Rev. **10**, 451 (2016).
[46] S. Wengerowsky, S. K. Joshi, F. Steinlechner, H. Hübel, and R. Ursin, An entanglement-based wavelengthmultiplexed quantum communication network, Nature (London) **564**, 225 (2018).
[47] M. Afzelius, C. Simon, H. de Riedmatten, and N. Gisin, Multimode quantum memory based on atomic frequency combs, Phys. Rev. A **79**, 052329 (2009).
[48] E. Saglamyurek *et al.*, A multiplexed light-matter interface for fibre-based quantum networks, Nat. Commun. **7**, 11202 (2016).
[49] A. Seri, A. Lenhard, D. Rielander, M. Gundogan, P. M. Ledingham, M. Mazzera, and H. de Riedmatten, Quantum Correlations Between Single Telecom Photons and a Multimode On-Demand Solid-State Quantum Memory, Phys. Rev. X **7**, 021028 (2017).
[50] D. V. Reddy and M. G. Raymer, Photonic temporal-mode multiplexing by quantum frequency conversion in a dichroic-finesse cavity, Opt. Express **26**, 28091 (2018).
[51] N. C. Menicucci, S. T. Flammia, and O. Pfister, One-Way Quantum Computing in the Optical Frequency Comb, Phys. Rev. Lett. **101**, 130501 (2008).
[52] T. Kobayashi, R. Ikuta, S. Yasui, S. Miki, T. Yamashita, H. Terai, T. Yamamoto, M. Koashi, and N. Imoto, Frequency-domain Hong-Ou-Mandel interference, Nat. Photonics **10**, 441 (2016).
[53] H.-H. Lu, J. M. Lukens, N. A. Peters, B. P. Williams, A. M. Weiner, and P. Lougovski, Quantum interference and correlation control of frequency-bin qubits, Optica **5**, 1455 (2018).
[54] R. Ikuta, Y. Kusaka, T. Kitano, H. Kato, T. Yamamoto, M. Koashi, and N. Imoto, Wide-band quantum interface for visible-to-telecommunication wavelength conversion, Nat. Commun. **2**, 537 (2011).
[55] J. M. Lukens and P. Lougovski, Frequency-encoded photonic qubits for scalable quantum information processing, Optica **4**, 8 (2017).
[56] R. Ikuta *et al.*, Polarization insensitive frequency conversion for an atom-photon entanglement distribution via a telecom network, Nat. Commun. **9**, 1997 (2018).